

## Electronic structure of $\alpha$ -Ga

Ch. S ndergaard,<sup>1</sup> Ch. Schultz,<sup>1</sup> S. Agergaard,<sup>1</sup> H. Li,<sup>1</sup> Z. Li,<sup>1</sup> S. V. Hoffmann,<sup>1</sup> Ch. Gr tter,<sup>2</sup> J. H. Bilgram,<sup>2</sup>  
and Ph. Hofmann<sup>1,\*</sup>

<sup>1</sup>*Institute for Storage Ring Facilities, University of Aarhus, DK-8000 Aarhus C, Denmark*

<sup>2</sup>*Laboratorium f r Festk rperphysik, Eidgen ssische Technische Hochschule, 8093 Z rich, Switzerland*

(Received 2 October 2002; revised manuscript received 14 January 2003; published 19 May 2003)

We have determined the electronic structure of  $\alpha$ -Ga using angle-resolved photoemission from the  $\alpha$ -Ga(010) surface. Data were collected both at 78 K and at 273 K, i.e., below and above the temperature of the surface phase transition. We observe a number of relatively flat bands reflecting the partly covalent character of  $\alpha$ -Ga. Our results agree fairly well with recent band-structure calculations.

DOI: 10.1103/PhysRevB.67.205105

PACS number(s): 71.20.Gj, 79.60.-i

$\alpha$ -Ga is an unusual elemental solid. On one hand, it is a metal, albeit with a low density of states at the Fermi energy. On the other hand, most of its properties are strikingly different from those of other metals. The crystal structure, shown in Fig. 1, is not a closed packed configuration but highly complicated. It is commonly described in terms of a face-centered orthorhombic unit cell containing eight atoms (space group  $Cmca$ ). It can also be described as a quasi-hexagonal unit cell containing only four atoms. This quasi-hexagonal character becomes particularly evident when looking at the Brillouin zone that is also shown in Fig. 1. Each gallium atom has only one nearest neighbor at a bonding distance of 2.44  . In fact, the crystal may also be viewed as having been constructed of  $Ga_2$  dimers as elemental building blocks.

This structure, which is identical to that of the molecular solids  $Br_2$  and  $I_2$ , suggests that  $\alpha$ -Ga is, apart from being a metal, at least to some degree also a covalently bonded solid. This view is supported by several other properties, for instance, the much higher electrical and thermal conductivity in the (010) plane (almost perpendicular to the dimers),<sup>1</sup> the sharp peaks in the optical reflectivity spectrum<sup>2</sup> and the low intensity at the Fermi level in angle-integrated photoemission.<sup>3,4</sup> A certain degree of covalency was also found in early theoretical work.<sup>5,6</sup> Gong and co-workers have recently pointed out that a good picture of the bonding in  $\alpha$ -Ga is to view it as a solid which is molecular and metallic at the same time.<sup>7</sup> The molecular properties are related to the presence of the  $Ga_2$  dimers, while the metallicity is present mainly in the so-called buckled planes that are created by the ends of the dimers and lie in the (010) planes, almost perpendicular to the dimer direction. This interpretation was based on the first-principles calculations of the electronic structure and was supported by a comparison to measured optical data. The calculated bands show a highly anisotropic Fermi surface, confirming earlier results, and very flat bands, similar to ‘‘molecular orbitals’’ along the (010) direction, i.e., almost parallel to the dimers.

In this paper, we present angle-resolved photoemission data taken in normal emission from the (010) surface of  $\alpha$ -Ga,<sup>8</sup> corresponding to the  $\Gamma$ - $\Sigma$ - $Z$  direction in the Brillouin zone and the region where the ‘‘molecular’’ character of the band structure should be most apparent. We find a number of

flat bands in good agreement with the most recent calculation of Bernasconi and co-workers<sup>9</sup> and we are able to confirm the picture of  $\alpha$ -Ga as a metallic molecular crystal.

Two truncated bulk structures are possible for the  $\alpha$ -Ga(010) surface, one with the dimers intact and one with the dimers broken. In addition to these, a third termination has been predicted in which the surface is reconstructed such that it is similar to epitaxially grown GaIII on  $\alpha$ -Ga.<sup>10</sup> At ambient temperature surface x-ray diffraction and low-energy electron diffraction (LEED) find the truncated-dimer termination to be present.<sup>11,12</sup> This is also consistent with the surface electronic structure.<sup>13</sup> Below 232 K, the surface undergoes a reconstructive phase transition to a  $(2\sqrt{2} \times \sqrt{2})R45^\circ$  structure.<sup>12,13,16</sup> LEED finds this structure to be

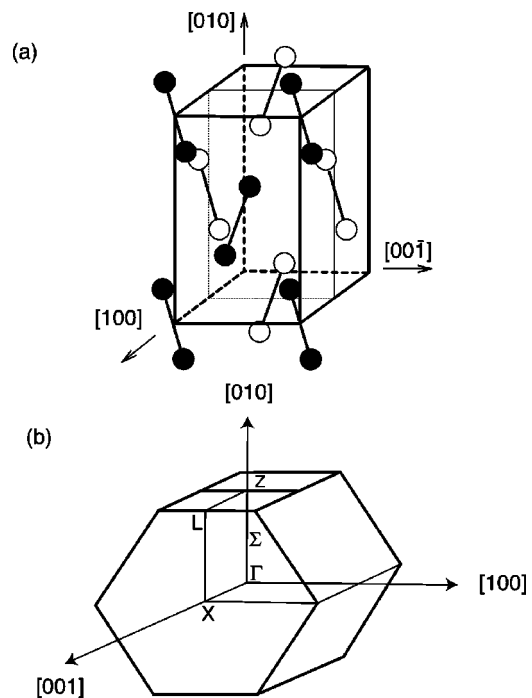


FIG. 1. (a) Orthorhombic unit cell of  $\alpha$ -Ga. The atoms are only drawn in half the unit cell for clarity reasons. The lines between the atoms indicate the shortest bond length in this structure. (b) Brillouin zone. Note that the Brillouin zone is rotated by  $90^\circ$  around the [010] axis with respect to the unit cell.

quite similar to the unreconstructed truncated-dimer surface.<sup>12</sup>

A key challenge in the preparation of clean  $\alpha$ -Ga surfaces is the low melting temperature of only  $T_m = 303$  K. This calls for special care when treating the crystal during polishing and *in situ* cleaning procedures. In particular, it is necessary to insert the sample into the vacuum system via a load lock, and it is not possible to anneal the surface to high temperatures (with respect to the bulk Debye temperature of 320 K). Nevertheless, it is possible to obtain clean and ordered surfaces with very wide terraces.<sup>14</sup> The  $\alpha$ -Ga(010) crystal surface used in this experiment was the natural (010) surface of a single-crystal grown by methods published previously.<sup>15</sup> The quality of this surface was further improved by mechanically polishing the crystal to mirror finish. After insertion into the vacuum system the surface was cleaned by sputtering with 0.5–2.0 keV  $\text{Ne}^+$  and “annealing” between 253 K and 273 K. This procedure resulted in a sharp ( $1 \times 1$ ) LEED pattern at 273 K. Every odd-integer spot in the [100] direction was missing, consistent with the bulk glide-plane symmetry. Surface cleanliness was checked by photoemission from the valence band and the Ga 3*d* core levels. In the initial stages of cleaning, monitoring the oxygen peak in the valence band proved useful. Oxygen gives rise to a broad peak at a binding energy of around 5.6 eV which does not disperse with emission angle or photon energy and is visible at all photon energies. Once this peak was not detectable any more and the Ga 3*d* spectra showed no indication of contamination-induced shoulders, the spectral shape of the surface state at  $\bar{C}$ <sup>16</sup> was found to be a more sensitive measure of the surface quality. The clean surface was found to be rather inert towards contamination. Only when kept at 35 K for more than 1 h, additional peaks at high binding energy were observable. We ascribe these to CO adsorption. The peaks could be removed by heating the sample to 78 K.<sup>17</sup>

Angle-resolved photoemission data were collected using the SGM-3 beamline at the storage ring ASTRID in Aarhus. A detailed description of the instrument will be given elsewhere.<sup>18</sup> In brief, the beamline, which is receiving its light from the undulator of ASTRID, covers an energy range from 14 eV to 140 eV with a resolving power better than 15 000. The electron spectrometer is a commercial hemispherical analyzer (VG-ARUPS10), which is mounted on a goniometer inside the chamber and equipped with a multi-channel detector. The total-energy resolution used in this work was better than 150 meV. The angular resolution was about  $\pm 0.7^\circ$ . The pressure during the experiments with synchrotron radiation was in the  $10^{-11}$  mbar range. All the data shown in this paper were measured in normal emission. The light was linearly polarized in the plane of incidence and incident  $40^\circ$  away of the surface normal towards the [101] direction.

In most cases, it is of an advantage to collect angle-resolved photoemission data at low temperatures. This reduces the amount of phonon-assisted indirect transitions (a final-state effect) and the broadening of the photoemission features by phonon scattering (an initial-state effect). It also facilitates the comparison to calculated band structures,

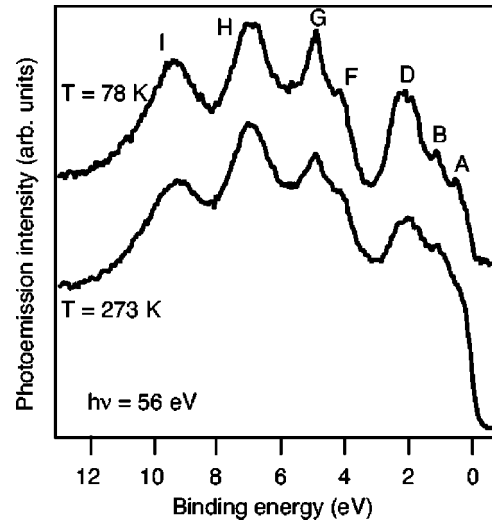


FIG. 2. Two normal-emission EDC's taken at a photon energy of 56 eV and two different temperatures. The peak labels correspond to the markers in Fig. 4.

which are usually not including the effects of finite temperature. In the present case, however, the situation is not so clear cut. The reason is the surface phase transition. Below 232 K the structure is  $(2\sqrt{2} \times \sqrt{2})R45^\circ$  and the new and shorter surface reciprocal-lattice vectors could lead to additional umklapp scattering, complicating the spectra. Therefore, we have collected two complete sets of data, one at 273 K and one at 78 K. Figure 2 shows two representative energy distribution curves (EDC's) taken with the same photon energy but at different temperatures. As expected, the high-temperature spectrum has a smaller peak to background ratio, caused by the decrease of coherent photoemission peaks at the expense of a higher incoherent background.<sup>19</sup> In addition to this the peaks appear to be slightly broader and less well resolved. This is particularly true for the two narrow features close to the Fermi energy at binding energies of 1.0 and 0.5 eV. The latter structure can only be seen in the low-temperature dataset. There appears to be almost no shift of the bands with temperature.

The complete low-temperature dataset is shown in Fig. 3. EDC's were taken in photon energy steps of 1 eV between  $h\nu = 22$  eV and 52 eV, and 2 eV for the higher energies. Below  $h\nu = 30$  eV a peak caused by the MVV Auger transition is visible at high binding energies. At all energies the peaks are clearly grouped into three regions with gaps between them. The first stretches from the Fermi level to a binding energy of 2.5 eV, the second from about 4 eV to 7.5 eV, and the third from 9 eV to 11 eV. It is also evident that several of the broader features must include more than one peak, in particular, for photon energies between 30 eV and 40 eV.

The analysis of the data proceeds by determining the position of the peaks and shoulders in every spectrum of the series, resulting in pairs of  $(E_{\text{bin}}, h\nu)$ . The key problem in the present type of experiment is the nonconservation of  $k_\perp$ , the wave-vector component perpendicular to the surface. This prevents us from a direct conversion of pairs  $(E_{\text{bin}}, h\nu)$  to the desired band structure, i.e., pairs of  $(E_{\text{bin}}, k)$ . How-

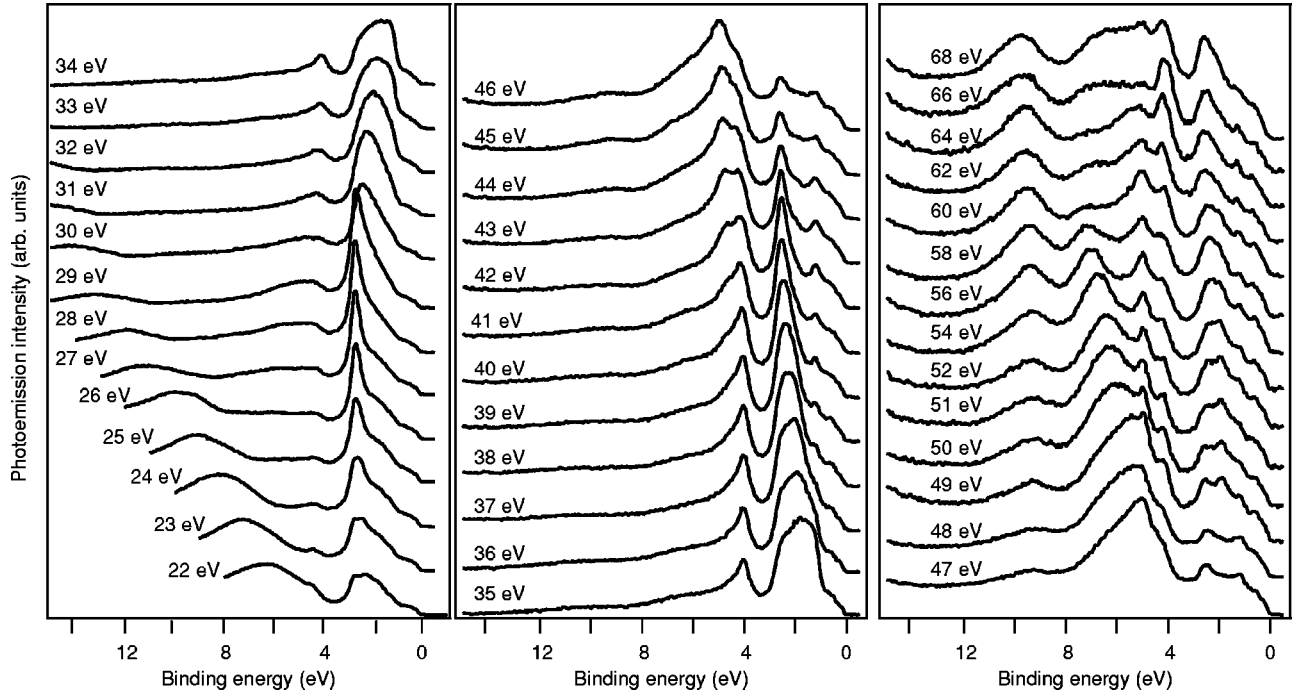


FIG. 3. EDC's taken at 78 K in normal emission as a function of photon energy. The EDC's are labeled by the photon energy.

ever, the parallel component of  $\vec{k}$  is conserved, and therefore it can at least be stated that the initial state lies on the  $\Gamma$ - $\Sigma$ - $Z$  line of the Brillouin zone. A common way of circumventing the problem is to simply assume a final-state dispersion, either by taking calculated final states or free-electronlike final states. We have attempted this by using a free-electron final-state dispersion of the form

$$E_f = \hbar^2(k_{\perp} + G)^2/2m^* + V_0, \quad (1)$$

where  $E_f$  is the final-state energy,  $G$  is a reciprocal-lattice vector,  $m^*$  is the effective electron mass, and  $V_0$  is the inner potential. The parameters for the final state were obtained by matching a free-electron parabola to the calculated "free-electronlike"  $\Sigma_1$  bands of Bernasconi *et al.*<sup>9</sup> in an extended zone scheme. We have used  $G = G_{220}$ ,  $m^* = 0.95m_e$ , and  $V_0 = -11.41$  eV. The resulting dispersions are displayed together with the calculated bands in Fig. 4.

Several conclusions can be drawn from the figure. First, we discuss what can be learned independently of the precise choice of final states, i.e., what we would have readily inferred from a plot of the  $(E_{\text{bin}}, h\nu)$ . The first thing is the position and the width of the bands. The second is the binding energy at certain high-symmetry points that are identified as extrema in the dispersion. To a lesser degree it can also be decided if a given peak is due to a surface state or a bulk state. A necessary condition for a peak to be a surface state is that its binding energy does not depend on  $k_{\perp}$ , i.e., that the peaks give rise to a flat band in a plot such as Fig. 4.

Three extrema are identified in Fig. 4: a binding-energy minimum of the  $C$  structure at  $k_{\perp} = 0.06 \text{ \AA}^{-1}$  ( $h\nu = 35$  eV), a minimum for the  $E$  structure at  $k_{\perp} = 0.04 \text{ \AA}^{-1}$

( $h\nu = 37$  eV) and a maximum for the  $H$  structure at  $k_{\perp} = 0.66 \text{ \AA}^{-1}$  ( $h\nu = 58$  eV). The structures  $A$  (only visible at low temperatures),  $D$ ,  $F$ , and  $G$  show little dispersion. Only the structure  $I$  disperses to higher binding energies for the highest photon energies (only taken for the sample at 273 K). An inspection of the calculated band structure in the  $\Gamma$ - $\Sigma$ - $Z$  direction<sup>9</sup> leads to the following tentative assignment of the structures. Guided by the absolute energy position of the bands, the binding-energy minima of the  $C$  and  $E$  structures are assigned to the  $\Gamma$  point, whereas the maximum of the  $H$  structure is assigned to the  $Z$  point. The measured binding energies at these points are in good agreement with the theory: The smallest binding energy of  $C$  is 1.35 eV and 1.4 eV for 78 K, and 273 K, respectively. The calculated band structure shows three bands in this energy region at  $\Gamma$ , at 0.85 eV, 1.62 eV, and 2.05 eV. The last band cannot be observed because of its symmetry (see below). It is conceivable that the two remaining bands give rise to the broad structure visible for photon energies around 35 eV and that our peak value represents only the most intense feature. The minimum binding energy for the  $E$  structure is at 3.9 eV and 3.85 eV for 78 K and 273 K, respectively. This fits very well with the calculated binding energy of the  $\Sigma_2$  band which is 3.9 eV. Finally, the maximum in the binding energy for the  $H$  structure is 7.1 eV and 7.05 eV for 78 K and 273 K, respectively, reached at a photon energy of 58 eV. For higher energies, the structure appears to disperse towards the Fermi level, but it also loses its intensity quickly. The calculated binding energy for this band at the  $Z$  point is 7.62 eV.

If we now focus on the detailed dispersion of the experimental bands in Fig. 4 and compare them to the calculation, we find a good agreement for the position of the high-symmetry points in the dispersion of the  $C$  and  $E$  bands. The

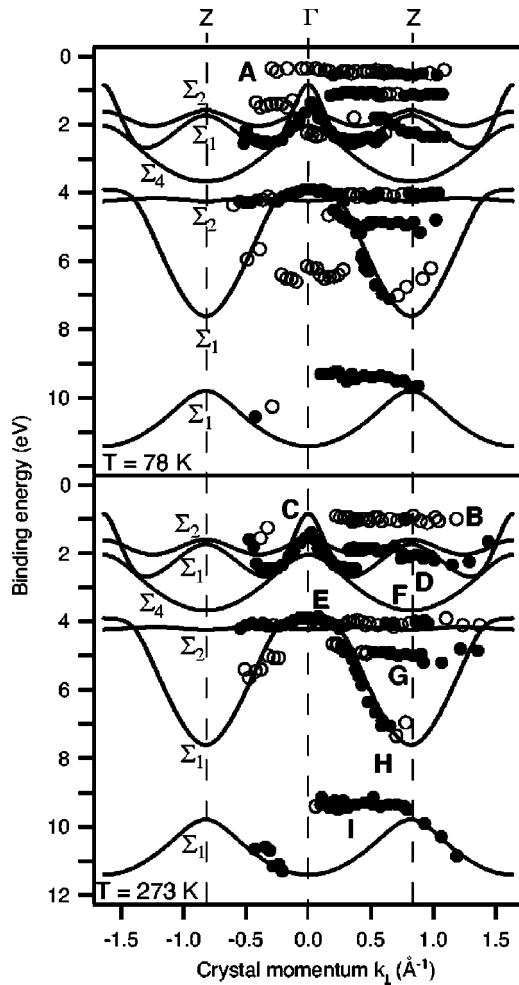


FIG. 4. Binding energy of the peaks (full circles) and shoulders (open circles) in the spectra plotted as a function of crystal momentum as determined by using free-electron final-states. The lines are the calculated band structure taken from Ref. 9.

maximum in the dispersion of the  $H$  band, however, is slightly shifted from the calculated position. We ascribe this to the failure of the free-electron model to adequately describe the final states. The main purpose of Fig. 4 is, however, to facilitate the comparison between measured and calculated bands and to show the qualitative differences and similarities away from the high-symmetry points.

With the aid of Fig. 4, we can proceed with the assignment of the yet unidentified features in the spectra. The state  $A$  is assigned to an electronic surface state. This identification is based on several facts. First of all, its binding energy does not change as the photon energy is varied. Second, it falls in a projected bulk band gap, as clearly seen by the calculated bands. Finally, a surface state at the same binding energy has been predicted to exist for the cut-dimer termination of this surface.<sup>10</sup> The fact that the  $A$  state is only observed in the low-temperature dataset could suggest that it is a feature from another part of the surface Brillouin zone, which has been scattered into the normal-emission direction by a reciprocal-lattice vector of the reconstruction. This

seems, however, unlikely because there is no obvious candidate for such state. More likely is that the weak  $A$  peak is simply hidden by the temperature-induced broadening of the other features and the increased background intensity at higher temperatures (see also Fig. 1).

The situation is less clear for the  $B$  state. As the  $A$  state, it also shows no dispersion with  $k_{\perp}$ . It does not fall into the region of the calculated band gap, but it has a smaller binding energy than all the measured states. So the most likely interpretation is that  $B$  is either another surface state, possibly only in a symmetry-induced gap, or a surface resonance.

The  $D$  and  $F$  states are interpreted as genuine bulk bands even though they, too, show very little dispersion. The narrow bands are, after all, characteristic for this direction in reciprocal space and the bands agree very well with the calculation. This is even seen in some detail, for example, by the fact that both the  $C$  and the  $D$  peaks are visible at  $k$  values, where the splitting of the highest  $\Sigma_1$  and  $\Sigma_2$  bands is largest.

In some details the agreement between experiment and calculation is less good. One is the presence of peaks that are not predicted by theory, in particular, the shoulder around 6 eV binding energy in the low-temperature data and the  $G$  structure. Such spurious structures can have several causes, for example, many-body effects or phonon-induced scattering, which gives rise to peaks at points of a high density of states. Neither of these scenarios seems very likely here. Another possibility is surface contamination. The  $G$  peak has a binding energy similar to an oxygen-induced peak but it is much narrower and invisible at low photon energies such that this explanation is also unlikely. Yet another possibility is that several structural phases are present on the surfaces. This, however, can be excluded by the good agreement between LEED simulations and experimental data.<sup>12</sup> From our data alone, it is hard to draw firm conclusions as to the origin of these peaks.

An even more pronounced difference between the experiment and the calculated band structure is the absence of the  $\Sigma_4$  band in the former. This is the main reason for the large gap we observe between the higher and lower bands. It is caused by the fact that photoemission from bands of  $\Sigma_4$  symmetry is forbidden in normal emission for any orientation of the polarization vector. To see this, consider the discussion of the symmetry properties of the (nonsymorphic) space group of  $\alpha$ -Ga, as presented by Slater *et al.*<sup>20</sup>

Finally, the highest binding energy  $\Sigma_1$  band is not observed over a large range of photon energies and where it has been observed, as the  $I$  band, its energy agrees only poorly with the calculation, except at the highest energies. This can be caused by two problems. One is the small cross section for this band and the other is that its energy falls in the region of gallium's plasmon and surface plasmon energies, which are 13 eV and 9 eV, respectively. Hence, a distortion of the spectra by a plasmon loss is conceivable. At lower photon energies the  $I$  band does not disperse at all and one might be tempted to assign it to a surface state in the lower projected band gap in the  $\Gamma$ - $Z$  direction. Such states have

been predicted for other terminations of this surface.<sup>10</sup> This assignment can be ruled out, however, because the state *does* disperse at higher energies. Moreover, it would be unusually broad for a surface state peak.

In conclusion, our experimental study of the electronic band structure of  $\alpha$ -Ga shows a good agreement with the most recent calculation of Bernasconi *et al.*<sup>9</sup> In particular, it confirms the presence of several rather flat bands in the  $\Gamma$ -Z

direction and is therefore consistent with the picture by Gong *et al.*,<sup>7</sup> which describes  $\alpha$ -Ga as a metallic molecular solid.

This work has been supported by the Danish National Research Council and the Carlsberg Foundation. H.L. thanks the Danish Foreign Ministry. We thank N. E. Christensen and M. Bernasconi for helpful discussions about the symmetry of  $\alpha$ -Ga.

---

\*Email address: philip@phys.au.dk; URL: <http://www.phys.au.dk/philip/>

<sup>1</sup>R.W. Powell, M.J. Woodman, and R.P. Tye, *Br. J. Appl. Phys.* **14**, 432 (1963).

<sup>2</sup>O. Hunderi and R. Rydberg, *J. Phys. F: Met. Phys.* **4**, 2084 (1974).

<sup>3</sup>F. Greuter and P. Oelhafen, *Zeitschrift für Physik B*, **34**, 123 (1979).

<sup>4</sup>S.R. Barman and D.D. Sarma, *Phys. Rev. B* **51**, 4007 (1995).

<sup>5</sup>W.A. Reed, *Phys. Rev.* **188**, 1184 (1969).

<sup>6</sup>V. Heine, *J. Phys. C* **1**, 222 (1968).

<sup>7</sup>X.G. Gong, G.L. Chiarotti, M. Parrinello, and E. Tosatti, *Phys. Rev. B* **43**, 14 277 (1991).

<sup>8</sup>Note that there are different conventions in use for the crystallographic directions in  $\alpha$ -Ga. We and Refs. 11–13,15,16 follow the crystallographic convention (*Cmca* symmetry), while Refs. 9,10,14 follow the historic (pseudotetragonal) convention. In the latter case the *b* and  $\bar{c}$  axes are reversed and the structure have the nonstandard *Mbab* symmetry. Our (010) surface corresponds to the (001) surface in this case.

<sup>9</sup>M. Bernasconi, G.L. Chiarotti, and E. Tosatti, *Phys. Rev. B* **52**, 9988 (1995).

<sup>10</sup>M. Bernasconi, G.L. Chiarotti, and E. Tosatti, *Phys. Rev. Lett.* **70**, 3295 (1993); M. Bernasconi, G.L. Chiarotti, and E. Tosatti, *Phys. Rev. B* **52**, 9999 (1995).

<sup>11</sup>D.A. Walko, I.K. Robinson, C. Grütter, and J.H. Bilgram, *Phys. Rev. Lett.* **81**, 626 (1998).

<sup>12</sup>S. Moré, E. A. Soares, M. A. Van Hove, S. Lizzit, A. Baraldi, Ch. Grütter, J. H. Bilgram, and Ph. Hofmann, *Phys. Rev. B* (to be published).

<sup>13</sup>Ch. Søndergaard, Ch. Schultz, S. Agergaard, S. V. Hoffmann, Z. Li, Ph. Hofmann, H. Li, Ch. Grütter, and J. H. Bilgram, *Phys. Rev. B* **67**, 165422 (2002).

<sup>14</sup>O. Züger and U. Dürig, *Ultramicroscopy* **42–44**, 520 (1992).

<sup>15</sup>R. Trittbach, C. Grütter, and J.H. Bilgram, *Phys. Rev. B* **50**, 2529 (1994).

<sup>16</sup>Ph. Hofmann, Y.Q. Cai, C. Grütter, and J.H. Bilgram, *Phys. Rev. Lett.* **81**, 1670 (1998).

<sup>17</sup>Ch. Søndergaard, Ph. D. thesis, University of Aarhus, 2001.

<sup>18</sup>S. V. Hoffmann, Ch. Søndergaard, Ch. Schultz, Z. Li, and Ph. Hofmann (unpublished).

<sup>19</sup>N.J. Shevchik, *J. Phys. C* **10**, L555 (1977).

<sup>20</sup>J.C. Slater, G.F. Koster, and J.H. Wood, *Phys. Rev.* **126**, 1307 (1962).